

# Journal of Materials Chemistry A

Accepted Manuscript



This is an *Accepted Manuscript*, which has been through the Royal Society of Chemistry peer review process and has been accepted for publication.

*Accepted Manuscripts* are published online shortly after acceptance, before technical editing, formatting and proof reading. Using this free service, authors can make their results available to the community, in citable form, before we publish the edited article. We will replace this *Accepted Manuscript* with the edited and formatted *Advance Article* as soon as it is available.

You can find more information about *Accepted Manuscripts* in the [Information for Authors](#).

Please note that technical editing may introduce minor changes to the text and/or graphics, which may alter content. The journal's standard [Terms & Conditions](#) and the [Ethical guidelines](#) still apply. In no event shall the Royal Society of Chemistry be held responsible for any errors or omissions in this *Accepted Manuscript* or any consequences arising from the use of any information it contains.

**Novel chelating material PS-ATD resin**  
applied to the efficient separation and recovery of  
platinum from aqueous solution



# Preparation of a novel chloromethylated polystyrene-2-Amino-1,3,4-thiadiazole chelating resin and its adsorption properties and mechanism for separation and recovery of Pt(IV) from aqueous solutions

Chunhua Xiong,\*<sup>a</sup> Yuqiang Zheng,<sup>a</sup> Yujie Feng,<sup>a</sup> Caiping Yao,<sup>a</sup> Chunan Ma,<sup>b</sup> Xuming Zheng<sup>c</sup> and Jianxiong Jiang<sup>d</sup>

<sup>a</sup> Department of Applied Chemistry, Zhejiang Gongshang University, Hangzhou, 310012, PR China

<sup>b</sup> State Key Laboratory Breeding Base of Green Chemistry-Synthesis Technology, Zhejiang University of Technology, Hangzhou, 310014, PR China

<sup>c</sup> Engineering Research Center for Eco-Dyeing & Finishing of Textiles, Ministry of Education, Zhejiang Sci-Tech University, Hangzhou, 310018, PR China

<sup>d</sup> Key laboratory of organosilicon chemistry and material technology, Ministry of Education, Hangzhou Normal University, Hangzhou, 311121, PR China

\*Corresponding author:

E-mail: [xiongch@163.com](mailto:xiongch@163.com) (C. Xiong);

Tel: +86-0571-88071024-7571;

Address: No.149 Jiaogong Road, Hangzhou, 310012, PR China

A novel chelating resin, chloromethylated polystyrene beads (PS-Cl) 2-Amino-1,3,4-thiadiazole (PS-ATD), with an efficient methodology was synthesized simply by the reaction of chloromethylated polystyrene with 2-Amino-1,3,4-thiadiazole. The effects of reaction parameters of PS-ATD resin (reaction solvent, reaction temperature and molar ratio of reagents and different time) were monitored to specify the best synthesis conditions. The functional group capacity (the content of the functional group) and the percentage conversion of the functional group of PS-ATD resin prepared under the optimum conditions were 3.65 mmol g<sup>-1</sup> and 88.6%, respectively. The structure of PS-ATD resin was characterized by elemental analysis, FTIR, TGA, SEM, and energy dispersive X-ray spectroscopy (EDS). Meanwhile, the adsorption properties of the resin for Pt(IV) were investigated by batch and column experiments. The results suggested that the resin possessed much better adsorption capability for Pt(IV) than for other metal ions and the maximum saturated adsorption capacity was 222.2 mg/g at 308 K, estimated from the Langmuir model. Furthermore, the resin could be regenerated through the desorption of the Pt(IV) anions using the mixture of 1 wt% Thiourea, 0.1 M HCl. Finally, The PS-ATD resin could provide a potential application for a efficient process of Pt(IV) recovery from aqueous solution.

## Introduction

Platinum group metals (PGM) have many important applications in different fields, such as technology, medicine and the automobile industry. Their excellent selectivity and activity towards reactants and resistance to oxidation at high temperatures make them very effective catalysts. For instance, platinum is a common active phase of petroleum cracking, dehydrogenation, reforming, and hydrogenation catalysts, which are extensively used in refining and petrochemical industries.<sup>1-2</sup> The demand for PGM in a car catalytic converter industry and jewellery sectors has been increasing for many years. Therefore, the recovery of the precious metals from the waste solutions and any secondary sources with low content of the desired metals became a very important economical and ecological issue.<sup>3-5</sup>

In the PGM recovery progress, Solvent extraction<sup>6</sup> is a traditional method. Alternatively, ion exchange,<sup>7-9</sup> membrane separation<sup>10</sup> and adsorption<sup>11</sup> have been developed for the recovery of PGM from solution. Comparatively, the adsorption seems to be the most suitable method for the recovery of PGM in the case of low concentration due to low cost, eco-friendly, and easy to handle, in addition, they have high enrichment factors, high recovery, and high selectivity for some metal ions.<sup>12-14</sup> Adsorption techniques using chelating resins have been widely applied in the fields of analytical chemistry and separation chemistry.<sup>15-17</sup> A chelating resin or polymer essentially consists of two components: the chelate forming functional group and the polymeric matrix or the support. Chelating or coordinating resins are polymers with covalently bound functional groups containing one or more donor atoms that are capable of forming complexes directly with metal ions, and the larger surface area is, the more efficient the chelating resin will be.<sup>18-19</sup> These polymers can also be used for a specific separation of one or more metal ions from solutions with different chemical environment.<sup>20</sup>

Chelating resins functionalized with synthetic or natural polymeric mixes were widely used to treat waste metals in a trace or ultra concentration range because of its low cost, high adsorption capacity, high recovery, and high selectivity for some metals ions.<sup>21-22</sup> The synthesis polymers containing heterocyclic functional groups, such as imidazole,<sup>23</sup> aminophosphonate,<sup>24</sup> quinoline,<sup>25</sup> pyridine,<sup>26</sup> imidazolylazo,<sup>27</sup> and 2-amino-2-thiazoline<sup>28</sup> have drawn a great deal of attention, for they have been practically applied in separation of trace metals from a variety of matrices. Macroporous chloromethylated polystyrene beads (PS-Cl) are an ideal polymeric matrix with a stable mechanical property. Active chloro- (Cl) present in polystyrene can be transformed into various new functional groups by special reactions. Heterocyclic ligands usually contain different kinds of donor atoms, and the electronic and steric effects of these atoms in the heterocyclic ligands may make them more selective for specific metal ion adsorption.<sup>29-33</sup> Resins functionalized with groups containing sulfur or nitrogen can be highly efficient in the selective adsorption of precious metals.<sup>34-35</sup>

In this work, a new chelating resin with 2-Amino-1,3,4-thiadiazole as functional group was synthesized and it was obtained by substitution reaction induced 2-Amino-1,3,4-thiadiazole onto PS-Cl. PS-ATD resin has a good adsorption capacity for Pt(IV) and a good application to the separation and recovery of Pt(IV) from multicomponent solutions with Fe(III), Zn(II), Cu(II), Ni(II), Cd(II) and Co(II). Some factors affecting adsorption, such as contact time, initial pH of solution, initial concentration of Pt(IV) and temperature have been examined. Static, dynamic adsorption and desorption process have also been examined. The experimental results afford a efficient pathway to the recovery of Pt(IV) from waste solutions and any secondary sources with low content of PGM in hydrometallurgical systems and fit in with the environmental protection.

## Experimental

## Materials

Chloromethyl polystyrene beads (PS-Cl) (cross-linked with 8% divinylbenzene (DVB), chlorine content 19.15%, specific surface area  $43\text{m}^2\text{ g}^{-1}$ ) was provided by Chemical Factory of NanKai University of China. 2-Amino-1,3,4-thiadiazole (ATD) was from Sinopharm Chemical Reagent Co., Ltd., China. Aqueous solutions of ions at various concentrations were prepared from  $\text{H}_2\text{P}_2\text{Cl}_6 \cdot 6\text{H}_2\text{O}$ ,  $\text{Fe}(\text{NO}_3)_3$ ,  $\text{Zn}(\text{NO}_3)_2 \cdot 6\text{H}_2\text{O}$ ,  $\text{CuCl}_2 \cdot 2\text{H}_2\text{O}$ ,  $\text{NiSO}_4 \cdot 6\text{H}_2\text{O}$ ,  $\text{Cd}(\text{NO}_3)_2 \cdot 4\text{H}_2\text{O}$ , and  $\text{CoCl}_2$  were used as sources for Pt(IV), Fe(III), Zn(II), Cu(II), Ni(II), Cd(II), and Co(II), respectively. All other reagents and solvents were of analytical reagent grade and were used without further purification.

## Synthesis of Resin

A 500 mL three-neck round-bottom flask was equipped with a condenser, thermometer, and nitrogen gas inlet tube. Thus, 1.0 g of PS-Cl beads and 175 mL of Toluene (TL) were added to the flask, swelling over night. Then, a certain amount of ATD and a small amount of metallic sodium used as catalyst were added to the flask. The system was swept with nitrogen to remove air, and then the reaction mixture was reacted by means of rotor stirring under nitrogen atmosphere at certain temperature. After completing the reaction, the resin was carefully washed thoroughly with TL and deionized water and then with acetone and ether. After that the obtained resin was dried in a vacuum at  $50\text{ }^\circ\text{C}$ . The conversion of the functional group of the resin synthesized can be calculated from the nitrogen content with the following equations:

$$F_c = \frac{N_c}{14 \times n_c} \times 1000 \quad (1)$$

$$X = \frac{F_n \times 1000}{1000 \times F_0 - \Delta m \times F_n \times F_0} \times 100\% \quad (2)$$

where  $F_0$  (mmol of Cl  $\text{g}^{-1}$ ) and  $F_c$  are the contents of the functional group of polystyrene and the synthesized resin, respectively;  $X$  is the functional group conversion (%);  $\Delta m$  is the incremental synthesis reaction resin ( $\text{g mol}^{-1}$ );  $n_c$  is the number of nitrogen atoms of ligand molecules, and  $N_c$  is the nitrogen content of the synthesized resin (%).

## Characterization

IR spectra for the samples were obtained from a Nicolet 380 Fourier transform infrared (FT-IR) spectrometer. Samples were dried before characterization by an infrared lamp to remove the adsorbed water. Thermogravimetric analysis was performed using a Mettler TGA (with a temperature range of  $25 - 1000\text{ }^\circ\text{C}$ , heating rate of  $20\text{ }^\circ\text{C min}^{-1}$ , and atmosphere of  $\text{N}_2$ ). Scanning electron micrographs for the samples were obtained from a HITACHI S-3000N scanning electron microscope (SEM). Spectra were obtained with an INCA ENERGY 350 system for energy dispersive X-ray spectroscopy (EDS). The specific surface area of the resins were determined on an Autosorb-1 automatic surface area and pore size analyzer.

## Resin adsorption and desorption experiments

Batch adsorption experiments were performed in conical flasks containing 30 mL of adsorption solution and 15.0 mg of dried PS-ATD resin. Adsorption of metal ions from aqueous solution to the adsorbents was studied at various pHs in Hydrochloric acid employed to control the pH of the solutions. After 24 h, the liquor samples were taken from the flask at appropriate time intervals. The residual concentration of the metal ions in the aqueous phases was determined by ICP. Adsorption isotherm studies were carried out with different initial Pt(IV) concentrations (3 mg/ 30 mL–9 mg/30 mL Pt(IV) solution). The kinetic experiments were carried out by means of the effect of contact time with time ranging from 2 to 20 h. The adsorption capacity ( $Q$ ,  $\text{mg g}^{-1}$ ) and distribution coefficient ( $D$ ,  $\text{mL g}^{-1}$ ) were calculated with the following formulas:

$$Q = \frac{C_0 - C_e}{W} V \quad (3)$$

$$D = \frac{C_0 - C_e}{W \cdot C_e} V \quad (4)$$

where  $C_0$  is the initial concentration in solution ( $\text{mg mL}^{-1}$ );  $C_e$  is the equilibrium concentration in solution ( $\text{mg mL}^{-1}$ );  $V$  is the volume of solution (mL); and  $W$  is the resin dry weight (g).

Desorption experiments were carried on following the completion of the adsorption experiments. After adsorption experiments, the resins were separated from the aqueous solution by filtration, washed by deionized water, and shaken with different eluent solutions of various concentrations at 298K for 24 h. After that time the concentration of Pt(IV) was similarly analyzed as described above. After each adsorption–desorption cycle, the resin beads were washed and reconditioned for adsorption in the succeeding cycle. The desorption ratio ( $E$ ) was calculated as follows:

$$E(\%) = \frac{C_d V_d}{(C_0 - C_e) V} \times 100\% \quad (5)$$

where  $C_d$  is the concentration of the solutes in the desorption solutions,  $V_d$  is the volume of the desorption solution, and  $C_0$ ,  $C_e$  and  $V$  are the same as defined above.

Continuous packed bed studies were performed in a fixed-bed mini glass column (3 mm  $\times$  30 cm long) with 100.0 mg of resin. The PS-ATD resin in the column was presoaked for 24 h before the experiment. The Pt(IV) solution at a known concentration and flow rate was passed continuously through the stationary bed of adsorbent in down-flow mode. The experiment continued until a constant Pt(IV) ion concentration was obtained. The column studies were performed at the optimum pH value determined from batch studies and at a constant temperature of 25 °C representative of environmentally relevant conditions.

### Instrumentation

The concentrations of metal ions were measured by Inductively Coupled Plasma Optical Emission Spectroscopy (ICP-OES). The elemental analysis was carried out by using a Gmbh Vario EL III elemental analyzer. A Mettler Toledo delta 320 pH meter was used for pH measurements. The samples were shaken in a DSHZ-300A temperature constant shaking machine. The water used in the present work was purified using a Mol research analysis type ultrapure water machine.

## Results and discussion

### Synthesis of PS-ATD resin

The effects of reactive solvent, the molar ratio of reagent and temperature on the yield of PS-ATD resin have been investigated, and optimal reaction condition has been found according to N content (N%) and functional group conversion (FGC, %). Reaction solvent has been identified as the most important variable governing the synthesis of resin. From the results, toluene is preferable compared with DMF and 1,4-dioxane according to N content (toluene, 15.040%; DMF, 7.819%; 1,4-dioxane, 7.508%) under 100 °C, for 12 h. The study temperature of ATD is in the range of 40–100 °C according with toluene boiling point 110.8 °C. Based on the above results, the optimum conditions are as follows: toluene as reaction solvent, reaction temperature of 100 °C and molar ratio of ATD to PS-Cl at 5:1 (Fig. 1a and b). The nitrogen contents and the functional group capacity of PS-ATD resin synthesized under the optimum condition are 15.040% and 3.65 mmol g<sup>-1</sup>, respectively.

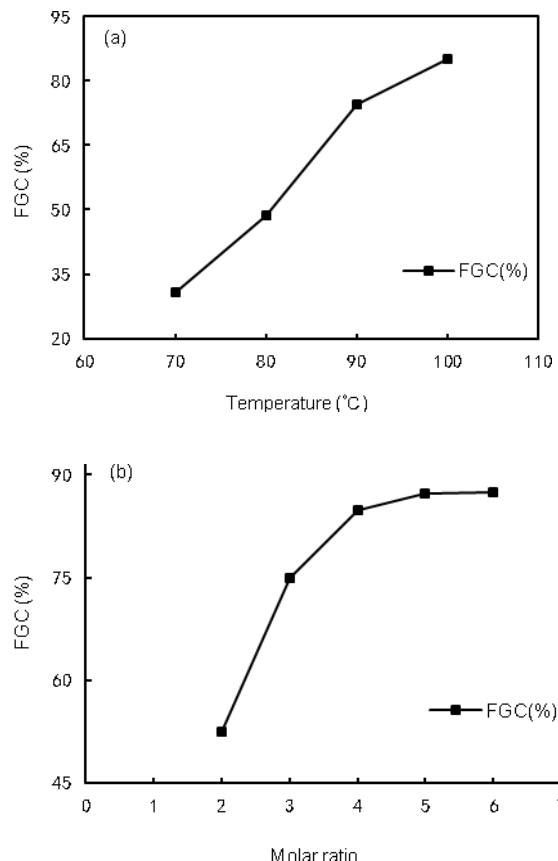


**Fig. 1** (a) Influence of temperature on N content (b) Influence of molar ratio on N content. 12 h, toluene, 100°C

### Characterization of resins

To identify the possibility of ATD bonding to PS-Cl resin, FT-IR spectra were obtained in Fig. 2. In general, it is observed that there are significant changes in the IR spectra of PS-Cl resin and PS-ATD resin. By comparison with the curve of PS-Cl resin, the characteristic peak of  $\text{CH}_2\text{-Cl}$  at  $1263$  and  $671\text{ cm}^{-1}$  disappeared in the curve of PS-ATD resin. In the spectra of PS-ATD resin, the characteristic bands of  $\text{-NH}_2$  at  $3350$  and  $3100\text{ cm}^{-1}$  disappeared, where a strong and broad characteristic band of secondary amine (N-H) peak at  $3400\text{ cm}^{-1}$  and the antisymmetric stretching vibration band at  $2924\text{ cm}^{-1}$  and symmetric stretching vibration band at  $2852\text{ cm}^{-1}$  of  $\text{-CH}_2$  groups appeared, confirmed the chemical modification of the PS-Cl resin and indicates the reaction between the  $\text{CH}_2\text{-Cl}$  and amino ligands. In addition, the PS-ATD resin was characterized by  $\nu_{\text{C=N}}$  at  $1623\text{ cm}^{-1}$ ,  $\nu_{\text{C-N}}$  at  $1512\text{ cm}^{-1}$ , and  $\nu_{\text{C-S}}$  at  $705\text{ cm}^{-1}$ , which suggests the presence of the thiazole rings introduced to the modified polymer<sup>36</sup>. The proposed synthesis route to the new prepared resin was presented schematically in Scheme 1. In the spectra of PS-ATD-Pt, the  $\nu_{\text{C=N}}$ ,  $\nu_{\text{C-N}}$ , and  $\nu_{\text{C-S}}$  stretching bands were shifted to lower wavenumbers by  $12\text{ cm}^{-1}$  (from  $1623$  to  $1611\text{ cm}^{-1}$ ),  $6\text{ cm}^{-1}$  (from  $1512$  to  $1506\text{ cm}^{-1}$ ), and  $7\text{ cm}^{-1}$  (from  $705$  to  $698\text{ cm}^{-1}$ ), respectively, which suggests that the nitrogens and sulfur in the thiazole ring were involved in Pt(IV) adsorption. In addition, the  $\nu_{\text{N-H}}$  stretching band decreased and shifted slightly (from  $3400$  to  $3405\text{ cm}^{-1}$ ), indicating that the secondary amine is also available in Pt(IV) binding process.

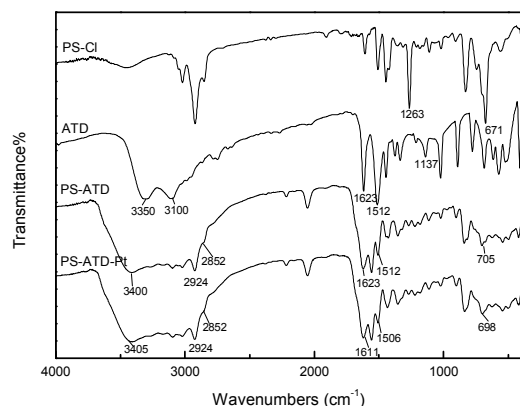
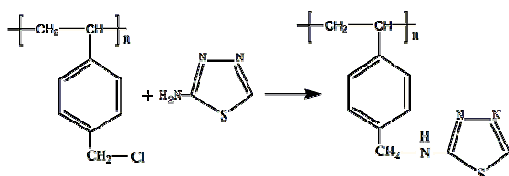


**Fig. 2** The infrared spectra of PS-Cl resin, ATD, PS-ATD resin and PS-ATD-Pt resin



**Scheme. 1** Proposed synthesis routes for PS-ATD resin

The thermal properties of ATD, PS-Cl, PS-ATD and PS-ATD-Pt was evaluated by thermogravimetric analysis (TGA) under a nitrogen atmosphere (Fig. 3). The decomposition of PS-Cl was a two-steps reaction. The first decomposition step, the temperature from 25°C to 480°C, the PS-Cl weight loss rate was about 27 wt%. According to the chlorine content of PS-Cl in the amount of 19.15%, Chloromethyl content (26.7%) in PS-Cl can be calculated. The weight loss of this step can be attributed to the fracture chloromethyl bond and residual moisture evaporation. In The second decomposition step, the temperature from 480°C to 1000°C, with 40% weight loss observed, which indicates that the skeleton structure of PS-Cl was broken. The remaining mass after heating was the char residue. ATD began to decompose at 200°C, the decomposition reached 100% at 950°C. As for PS-ATD, two weight losses were obtained. The first weight loss occurred from 25°C to 460°C, due to the decomposition of ATD and the breaking of covalent bond between PS-Cl and ATD. The second case, which occurs at about 460°C, PS-ATD did a further decomposition, and the weight loss rate reached 72.3wt% at 1000°C. Similar to PS-ATD, the TGA curve of PS-ATD-Pt also included two steps. Compared to the weight loss rate of the PS-ATD, the weight loss rate of PS-ATD-Pt was slightly less than 20 wt%. According to the adsorption of platinum on PS-ATD, it could be calculated that the content of platinum in PS-ATD-Pt resin was about 20 wt%. Therefore, the 52wt% of the weight loss rate at 1000°C was the char residue and platinum.

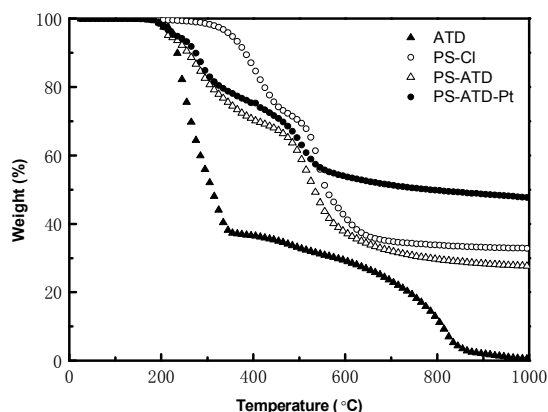


Fig. 3 TGA curves of ATD, PS-Cl resin, PS-ATD resin and PS-ATD-Pt resin.

BET (Brunauer–Emmett–Teller) experiments were conducted using nitrogen adsorption at 77.35 K. PS-ATD resin was calcined at 130°C for 10 h under a vacuum, and the nitrogen sorption experiments were performed. BET measurement showed that the surface area of the PS-ATD resin was 28.648 m<sup>2</sup>g<sup>-1</sup>. Compared with PS-Cl resin, the surface area diminished due to the surface of the PS-Cl resin partly covered with the ATD. Therefore, the significantly higher surface area was not the only factor responsible for the higher adsorption capacity, and the existence of ATD could be critical.

Fig 4 is SEM images of the morphology and surface composition of PS-ATD resin and PS-ATD-Pt resin. The synthesized resin was supplied in the form of regular spheres. Compared Fig 4(a) with Fig 4(c), it can be found that the smooth surface of PS-ATD resin turned thicker and coarser just like the granular flake material. In order to confirm the presence of Pt(IV) in PS-ATD-Pt resin, EDS spectrum of the PS-ATD-Pt resin was investigated in Fig 5. The peak indicating the presence of platinum can be clearly observed. Hence, the results revealed that Pt(IV) was loaded on the surface of PS-ATD-Pt resin, which was consistent with the results of SEM.

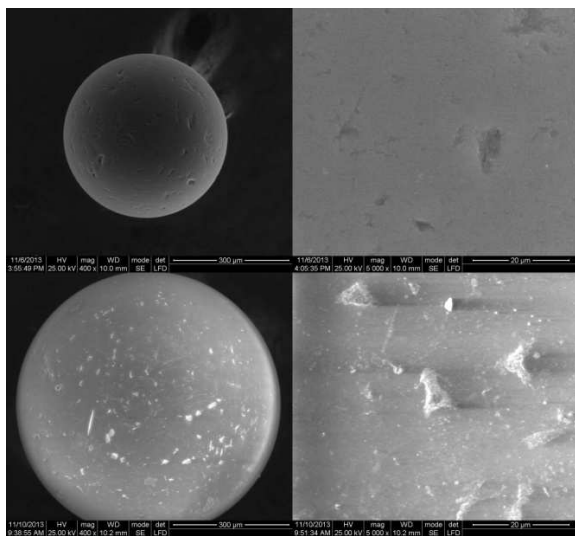


Fig. 4 SEM images of PS-ATD resin and PS-ATD-Pt resin. (a) PS-ATD resin at a magnification of 400; (b) PS-ATD resin at a magnification of 5000; (c) PS-ATD-Pt resin at a magnification of 400; (d) PS-ATD-Pt resin at a magnification of 5000.

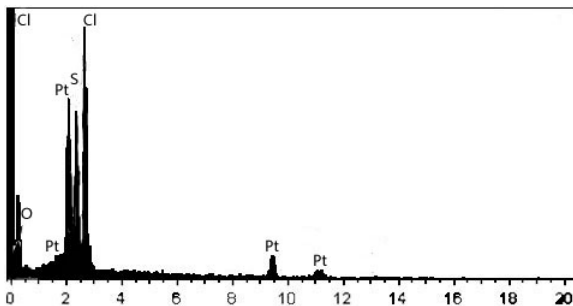


Fig. 5 EDS spectrum of PS-ATD-Pt resin.

### Influence of pH on the sorption of six metal ions

The pH of an aqueous solution is one of the most important factors for metal–chelate formation and in solid phase extraction processes. In view of it, the influence of pH on the adsorption behavior of PS-ATD resin for Pt(IV), Fe(III), Zn(II), Cu(II), Ni(II), Cd(II), and Co(II) metal ions was investigated in the range  $H^+ 10^{-3}$ - $2 \text{ mol L}^{-1}$  using hydrochloric acid solution. The results were shown in Fig. 6. It can be noted that the adsorption capacity of PS-ATD resin for Pt(IV) ion was far greater than for other metal ions, suggesting that Pt(IV) ion can be easily separated from these metal ions using PS-ATD resin. Besides, pH has little effect on the Pt(IV) adsorption capacity, which can predict the PS-ATD resin can be widely applied to enrichment and recovery of platinum in different pH solution. The highest adsorption capacity for Pt(IV) was  $215.7 \text{ mg g}^{-1}$  at pH 1 in the hydrochloric acid solution. Therefore, pH 1 was selected for subsequent studies.

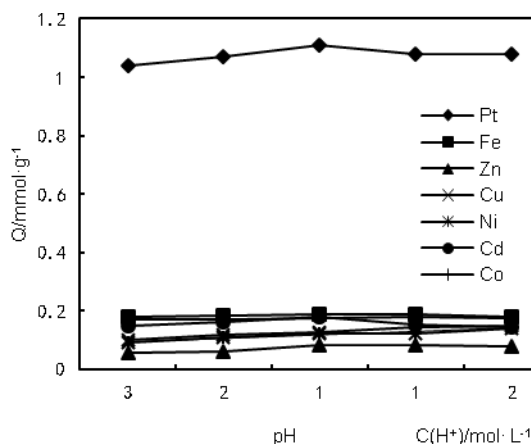


Fig. 6 The capacity of PS-ATD resin in different pH and  $C(H^+)$ , metal ions  $5.0 \text{ mg}/30.0\text{ml}$ ,  $15.0\text{mg}$  ATDR resin, at  $298 \text{ K}$ ,  $100 \text{ rpm}$ .

### Adsorption kinetics

The influence of the contact time on the adsorption of Pt(IV) was studied in the time range 2–40 h under pH 1 at 288, 298, and 308 K. The change in the uptake of Pt(IV) by the resin was shown in Fig. 7. It is clear that Pt(IV) was adsorbed rapidly at different temperatures within a few hours, and then absorption increased slowly until the equilibrium state was reached at 15 h. After 15 h, the amount of Pt(IV) adsorption did not increase further in contact time. As seen here, the equilibrium adsorption capacity increased within the range of reaction temperature (288–308 K), which illustrates that higher temperature favored the adsorption of Pt(IV) onto the adsorbent. This influence suggests that the mechanism associated with Pt(IV) adsorption onto PS-ATD resin involves a temperature-dependent process.

Several kinetic models were available to examine the controlling mechanism of adsorption from a liquid phase on the PS-ATD resin and to interpret the experimental data obtained. The kinetics of adsorption can be described by the Lagergren first-order rate expression<sup>37-38</sup> and pseudo second-order kinetic model equation<sup>39-40</sup> that were given by:

$$\ln(Q_e - Q_t) = \ln Q_1 - k_1 t \quad (6)$$

$$\frac{t}{Q_t} = \frac{1}{k_2 Q_2^2} + \frac{t}{Q_2} \quad (7)$$

where  $Q_e$  and  $Q_t$  are the amounts of Pt(IV) adsorbed on the adsorbent at equilibrium ( $\text{mg g}^{-1}$ );  $Q_1$  and  $Q_2$  are the adsorption capacity of the Lagergren first-order model and the pseudo second-order model ( $\text{mg g}^{-1}$ ), respectively;  $k_1$  and  $k_2$  are the rate constant of the Lagergren first-order model ( $\text{h}^{-1}$ ) and the pseudo second-order model ( $\text{g mg}^{-1} \text{h}^{-1}$ ). The fitting validity of these models is traditionally verified by the linear plots of  $\ln(Q_e - Q_t)$  versus  $t$ , and  $t/Q_t$  versus  $t$ , respectively. The correlation coefficient  $R_2^2$  for the pseudo second-order equation was better than the correlation coefficient  $R_1^2$  for the Lagergren first-order equation. Moreover, the experimental-calculated capacity of the pseudo second-order model produces alternatives, as observed in Table 1. Therefore, the adsorption behavior of Pt(IV) on PS-ATD resin can be perfectly explained by pseudo second-order mechanism, which means the chemical adsorption is the rate-controlling step<sup>41</sup>.

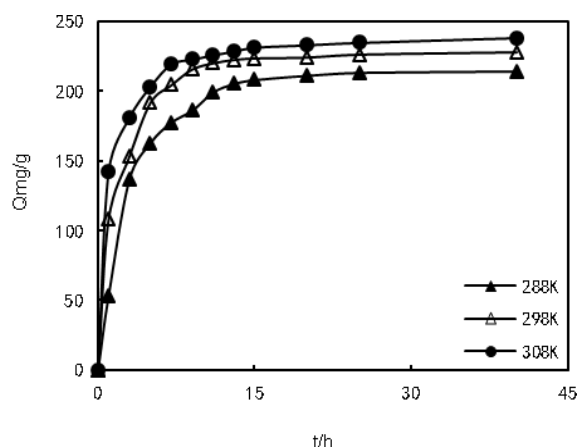


**Fig. 7** Adsorption kinetics and capacity  $Q$  at different times and different temperatures, metal ions 5.0 mg/30.0ml, 15.0mg PS-ATD resin, at 298 K, pH 1, 100 rpm.

**Table 1** Kinetics model constants for adsorption of Pt(IV) by PS-ATD resin

$T(\text{K})$	$Q_e(\text{mg g}^{-1})$	Lagergren first-order			Pseudo second-order		
		$K_1(\text{h}^{-1})$	$Q_1(\text{mg g}^{-1})$	$R_1^2$	$K_2(\text{g mg}^{-1} \text{h}^{-1})$	$Q_2(\text{mg g}^{-1})$	$R_2^2$
288	214	0.21	155	0.9908	$1.7 \times 10^{-3}$	238	0.9967
298	228	0.18	86	0.9156	$3.5 \times 10^{-3}$	239	0.9991
308	238	0.14	68	0.9217	$4.8 \times 10^{-3}$	244	0.9998

### Adsorption Isotherms

To further explore the adsorption mechanism, we used Langmuir<sup>42</sup> and Freundlich<sup>43</sup> isotherm models to analyze the equilibrium data for the experiments carried out at different temperature under pH 1. Langmuir and Freundlich equations are the widely used in equilibrium-based isotherm models. The linear form of the Langmuir isotherm was represented by the following equation:

$$\frac{C_e}{Q_e} = \frac{1}{Q_m K_L} + \frac{C_e}{Q_m} \quad (8)$$

$$\log Q_e = \frac{1}{n} \log C_e + \log K_F \quad (9)$$

where  $Q_m$  is the maximal adsorption capacity ( $\text{mg g}^{-1}$ ),  $Q_e$  is the equilibrium Pt(IV) concentration on the adsorbent ( $\text{mg g}^{-1}$ ), and  $K_L$  is the Langmuir constant.  $K_F$  is the Freundlich constant and  $n$  is an empirical constant related to the magnitude of the adsorption driving force. The linear Langmuir and Freundlich plots may be obtained by plotting  $C_e/Q_e$  versus  $C_e$  and  $\log Q_e$  versus  $\log C_e$ , respectively. The data in Table 2 present the results along with associated correlation coefficients  $R^2$ . They reveal that the adsorption of Pt(IV) onto PS-ATD resin was fitted better to the Langmuir model than the Freundlich model at investigated temperatures. Those results indicated that the adsorption of Pt(IV) onto PS-ATD resin was a monolayer type — a layer of metal ions on the adsorbent surface appeared. The increase of the  $Q_m$  value with the temperature rising signified that the process needed thermal energy (endothermic) and that there was a chemical interaction between adsorbent and adsorbate.

**Table 2** Parameters for adsorption isotherms of Pt(IV) by PS-ATD resin

T(K)	Langmuir			Freundlich		
	$Q_m(\text{mg g}^{-1})$	$K_L(\text{mL mg}^{-1})$	$R^2$	$1/n$	$K_F((\text{mg g}^{-1})/(\text{mg mL}^{-1})^{1/n})$	$R^2$
288	149.3	83.7	0.9984	0.067	157.1	0.9022
298	196.1	169.9	0.9994	0.041	201.4	0.937
308	222.2	225.1	0.9996	0.035	228.7	0.9302

### Thermodynamic parameters

In any adsorption procedure, both energy and entropy considerations should be taken into account in order to determine which process will take place spontaneously. The amounts of Pt(IV) ions adsorbed at equilibrium at different temperatures, which were 288, 298 and 308K, have been examined to obtain thermodynamic parameters for the adsorption system. The changes in the Gibbs free energy ( $\Delta G$ ), enthalpy ( $\Delta H$ ) and entropy ( $\Delta S$ ) for the adsorption process can be determined by using following equations:<sup>44</sup>

$$\Delta S = (\Delta H - \Delta G) / T \quad (10)$$

$$\ln K_d = -\frac{\Delta H}{RT} + \frac{\Delta S}{R} \quad (11)$$

where  $R$  is the gas constant and  $T$  is the absolute temperature as mentioned in Arrhenius equation.  $K_d$  is the distribution coefficient of the adsorbate ( $Q_e/C_e$ ). The plot of  $\ln K_d$  versus  $1/T$  gives the straight line form which  $\Delta H$  and  $\Delta S$  is calculated based on the slope and intercept of the linear form. The negative value of  $\Delta G$  ( $-41.9$  to  $-45.6 \text{ kJ mol}^{-1}$ ) confirms the spontaneity of the adsorption process with increasing temperature and the positive value of  $\Delta H$  ( $9.9 \text{ kJ mol}^{-1}$ ) suggests that the adsorption was endothermic in nature. In addition, the value of  $\Delta S$  ( $108.2 \text{ J K}^{-1} \text{ mol}^{-1}$ ) was found to be positive due to the exchanged of the metal ions with more mobile ions present on the exchanger, which would cause increase in the entropy, during the adsorption process.<sup>45</sup>

### Desorption and Regeneration Studies

Whether an adsorbent is economically attractive in the removal of metal ions from aqueous solution depends not only on the adsorptive capacity, but also on how well the adsorbent can be regenerated and used again. For repeated use of an adsorbent, adsorbed metal ions should be easily desorbed under suitable conditions. Desorption of the adsorbed Pt(IV) from PS-ATD-Pt resin was studied by the batch method using various concentrations of thiourea, HCl and

thiourea–HCl solutions. The results were presented in Table 3. It was found that 1 wt% thiourea–0.5 M HCl solution provided effectiveness of the desorption of Pt(IV) from PS-ATD-Pt resin. The amount of adsorption of Pt(IV) was not significantly changed up to 5 cycles and the desorption efficiencies were above 96%. Therefore, the adsorbent material could be successfully applied for the recovery of Pt(IV) from aqueous solution.

**Table 3** Parameters for desorption efficiency of Pt(IV) by PS-ATD resin

Desorption agent	0.5 wt% thiourea	1 wt% thiourea	2 wt% thiourea	5 wt% thiourea	0.5 M HCl	1.0 M HCl	1.5 M HCl	0.5M HCl-1wt% thiourea
Desorption efficiency(%)	63.68	89.24	72.89	64.05	47.54	36.22	32.36	99.91

### Dynamic Adsorption and Desorption

Batch experimental data are often difficult to apply directly to fixed-bed adsorption because isotherms are unable to give accurate data for a dynamically operated column. The fixed-bed column operation allows more efficient utilization of the adsorptive capacity than the batch process. The total adsorption quantity of Pt(IV)  $Q$  ( $\text{mg g}^{-1}$ ) in the column for a given feed concentration and flow rate can be calculated from equation:<sup>46</sup>

$$Q = \int_0^v \frac{(C_0 - C_e)}{m} dV \quad (12)$$

where  $C_0$  and  $C_e$  are metal ion concentrations in the influent and effluent, respectively,  $m$  is the total weight of the adsorbent loaded in the column, and  $v$  is the volume of metal solution passed through the column. The capacity value  $Q$  was obtained by graphical integration as  $209.8 \text{ mg g}^{-1}$ . Successful design of a column sorption process requires prediction of the concentration time profile or breakthrough curve for the effluent. Traditionally, the Thomas model is used to fulfill the purpose. The model has the following form:<sup>47</sup>

$$\ln\left(\frac{C_0}{C_e} - 1\right) = \frac{K_T Q m}{\theta} - \frac{K_T C_0}{\theta} V \quad (13)$$

where  $K_T$  is the Thomas rate constant ( $\text{mL min}^{-1} \text{ mg}^{-1}$ ),  $\theta$  is the volumetric flow rate ( $\text{mL min}^{-1}$ ), and  $m$  is the mass of the resin (g). The kinetics coefficient  $K_T$  and the adsorption capacity  $Q$  of the column can be determined from a plot of  $\ln[(C_0/C_e)-1]$  versus  $1/\theta$  at a certain flow rate. The Thomas equation coefficient for Pt(IV) adsorption was  $K_T = 2.25 \times 10^{-2} \text{ mL min}^{-1} \text{ mg}^{-1}$  and  $Q = 211.7 \text{ mg g}^{-1}$ . The theoretical predictions based on the model parameters were compared with the observed data as shown in Fig 8. It was showed that the experimental data were well fitted by the Thomas model with a high  $R^2$  value (0.9756).

With respect to the dynamic desorption of Pt(IV) from PS-ATD-Pt resin, the 1 wt% thiourea–0.5 M HCl eluent was employed. The desorption curve was plotted with the effluent concentration ( $C_e$ ) versus elution volume ( $V$ ) from the column at a flow rate of  $0.1 \text{ ml min}^{-1}$  less than the adsorption flow rate so that the volume of elution was less, which was helpful in easy handling of the metal ions. As shown in Fig 9, a sharp increase of Pt(IV) concentration at the beginning of acid elution was observed, the total volume of eluent was 20 mL and desorption process took 3.3 h, after which further desorption was negligible. Therefore, the 1 wt% thiourea–0.5 M HCl eluent could help in easy handling and removal of Pt(IV).

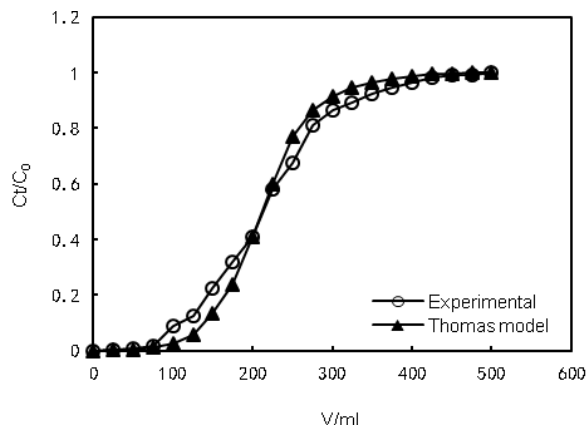


**Fig. 8** Experimental and predicted breakthrough curves using Thomas model for Pt(IV) adsorption by PS-ATD resin ,at 298 K, pH 1, 100 rpm.

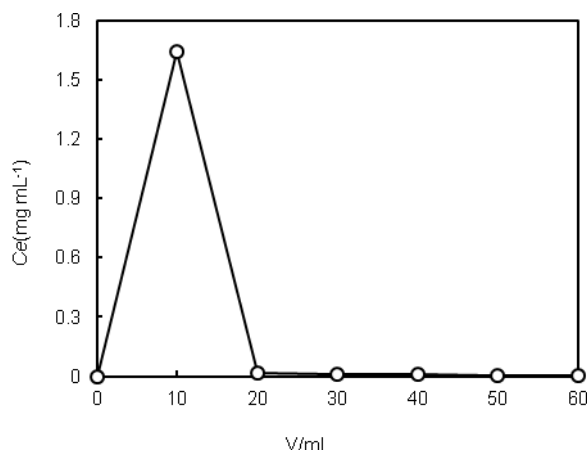


**Fig. 9** Dynamic desorption curve flow rate = 0.1 mL/min.

## Conclusions

In the research, a new composite chelating resin which has N donor atoms and S donor atoms have been synthesized. FTIR, elemental, TGA, BET, SEM and EDS results indicate that the immobilization of ATD onto PS-Cl is accomplished. The material offers the versatility to complex different metal ions due to the presence of the ligand. Furthermore, the results of the present investigation shows that PS-ATD resin is a potentially useful adsorbent for the separation of Pt(IV) ions from mixed solution. The kinetics of adsorption of Pt(IV) on PS-ATD resin are complex and while the results are tested with models based on the Lagergren first-order and pseudo second-order, close conformity could be obtained with pseudo second-order mechanism. It is evident from the experimental data that the adsorption of Pt(IV) ions onto PS-ATD resin fitted better with Langmuir isotherm model than Freundlich isotherm models. The adsorption process is endothermic and spontaneous at ambient higher temperature. Meanwhile, Thomas model is applied to experimental data obtained from dynamic studies performed on fixed column to predict the breakthrough curves and to determine the column kinetic parameters. In conclusion, PS-ATD resin can satisfactorily be considered as an alternative application for separation and recovery of Pt(IV) from aqueous solution.

## Acknowledgements

The work is supported by the National Science Fundamental Project of China (No. 20972138), the Ph.D. Programs

Foundation of Ministry of Education of China (No. 20133326110006), and the Open Foundation of Zhejiang Provincial Top Key Academic Discipline of Applied Chemistry and Eco-Dyeing & Finishing Engineering (No. YR2012010).

## References

- 1 S. W. Won, J. Mao, I.-S. Kwak, M. Sathishkumar and Y.-S. Yun, *Bioresource Technol*, 2010, **101**, 1135-1140.
- 2 R. S. Marinho, C. N. da Silva, J. C. Afonso and J. W. S. D. da Cunha, *J Hazard Mater*, 2011, **192**, 1155-1160.
- 3 B. K. Reck and T. Graedel, *Science*, 2012, **337**, 690-695.
- 4 R. Mulholland and A. Turner, *Environmental Pollution*, **2011**, 159, 977-982.
- 5 D. Jermakowicz-Bartkowiak, *Reactive and Functional Polymers*, 2007, **67**, 1505-1514
- 6 J.E. Barnes, J.D. Edwards, *Chem. Ind*, 1982, **6**, 151.
- 7 K. Jainae, K. Sanuwong, J. Nuangjamnong, N. Sukpirom and F. Unob, *Chem Eng J*, 2010, **160**, 586-593.
- 8 S. Tanaka, A. Harada, S. Nishihama and K. Yoshizuka, *Sep Sci Technol*, 2012, **47**, 1369-1373.
- 9 E.R. Els, L. Lorenzen, C. Aldrich, *Min. Eng*, 2000, **13**, 401
- 10 K. Takahiko, G. Masahiro, N. Fumiyuki, *J. Membr. Sci*, 1996, **120**, 77.
- 11 X. Q. Chen, K. F. Lam, S. F. Mak and K. L. Yeung, *J Hazard Mater*, 2011, **186**, 902-910.
- 12 H.-w. Ma, X.-p. Liao, X. Liu and B. Shi, *Journal of membrane science*, 2006, **278**, 373-380.
- 13 C. H. Xiong, X. Y. Chen and C. P. Yao, *Curr Org Chem*, 2012, **16**, 1942-1948.
- 14 L. Q. Yang, Y. F. Li, X. L. Jin, Z. F. Ye, X. J. Ma, L. Y. Wang and Y. P. Liu, *Chem Eng J*, 2011, **168**, 115-124.
- 15 Y. Baba, Y. Aoya, K. Ohe, S. Nakamura and T. Ohshima, *Journal of chemical engineering of Japan*, 2005, **38**, 887-893.
- 16 E. Guibal, M. Ruiz, T. Vincent, A. Sastre and R. Navarro-Mendoza, *Sep Sci Technol*, 2001, **36**, 1017-1040.
- 17 E. Guibal, N. Von Offenberg Sweeney, T. Vincent and J. Tobin, *Reactive and Functional Polymers*, 2002, **50**, 149-163.
- 18 M. R. Gandhi, N. Viswanathan and S. Meenakshi, *Ind Eng Chem Res*, 2012, **51**, 5677-5684.
- 19 L. J. Li, F. Q. Liu, X. S. Jing, P. P. Ling and A. M. Li, *Water Res*, 2011, **45**, 1177-1188.
- 20 E. Birinci, M. Gulfen and A. O. Aydin, *Hydrometallurgy*, 2009, **95**, 15-21.
- 21 C. Er, B. F. Senkal and M. Yaman, *Food Chem*, 2013, **137**, 55-61.
- 22 F. Pagnanelli, S. Mainelli, L. Bornoroni, D. Dionisi and L. Toro, *Chemosphere*, 2009, **75**, 1028-1034.
- 23 C. X. Li, J. T. Dou, J. J. Cao, Z. Q. Li, W. K. Chen, Q. Z. Zhu and C. F. Zhu, *J Organomet Chem*, 2013, **727**, 37-43.
- 24 S. K. Pang and K. C. Yung, *Ind Eng Chem Res*, 2013, **52**, 2418-2424.
- 25 B. Ara, Z. Y. Chen, J. Shah, M. R. Jan and L. Ye, *J Appl Polym Sci*, 2012, **126**, 315-321.
- 26 R. Saha, S. Das, A. Banerjee, A. Sahana, M. Sudarsan, A. M. Z. Slawin, Y. Li and D. Das, *J Hazard Mater*, 2010, **181**, 154-160.
- 27 S. Pramanik, P. K. Dhara and P. Chattopadhyay, *Talanta*, 2004, **63**, 485-490.
- 28 Y. Chen and Y. Zhao, *Reactive and Functional Polymers*, 2003, **55**, 89-98.
- 29 C. H. Xiong, X. Y. Chen and X. Z. Liu, *Chem Eng J*, 2012, **203**, 115-122.
- 30 C. N. Ji, S. H. Song, C. R. Wang, C. M. Sun, R. J. Qu, C. H. Wang and H. Chen, *Chem Eng J*, 2010, **165**, 573-580.
- 31 C. Xiong and C. Yao, *Chem Eng J*, 2009, **155**, 844-850.
- 32 G. Zong, H. Chen, R. Qu, C. Wang and N. Ji, *J Hazard Mater*, 2011, **186**, 614-621.
- 33 R. Qu, C. Wang, C. Sun, C. Ji, G. Cheng, X. Wang and G. Xu, *J Appl Polym Sci*, 2004, **92**, 1646-1652.
- 34 M. Yıldırım and İ. Kaya, *Synthetic Met*, 2012, **162**, 436-443.
- 35 C. Xiong, Q. Jia, X. Chen, G. Wang and C. Yao, *Ind Eng Chem Res*, 2013, **52**, 4978-4986.
- 36 S. Saydam and E. Yilmaz, *Spectrochimica Acta Part A: Molecular and Biomolecular Spectroscopy*, 2006, **63**, 506-510.
- 37 Y. Ho and G. McKay, *Water Res*, 1999, **33**, 578-584.
- 38 O. Keskinan, M. Goksu, M. Basibuyuk and C. Forster, *Bioresource Technol*, 2004, **92**, 197-200.
- 39 C.-T. Tien and C. Huang, *Trace Metals in the Environmental. 1. Heavy Metals in the Environment*, 1991, **3**, 295-311.
- 40 Y. Ho and G. McKay, *Process Safety and Environmental Protection*, 1999, **77**, 165-173.
- 41 M. Monier and D. Abdel-Latif, *J Hazard Mater*, 2013.
- 42 I. Langmuir, *J Am Chem Soc*, 1918, **40**, 1361-1403.
- 43 H. Freundlich, *Engelmann, Leipzig*, 1906.
- 44 N. Ünlü and M. Ersoz, *J Hazard Mater*, 2006, **136**, 272-280.
- 45 S. Sen Gupta and K. G. Bhattacharyya, *J Environ Manage*, 2008, **87**, 46-58.
- 46 M. Tabakci and M. Yilmaz, *J Hazard Mater*, 2008, **151**, 331-338.
- 47 T. Mathialagan and T. Viraraghavan, *J Hazard Mater*, 2002, **94**, 291-303.